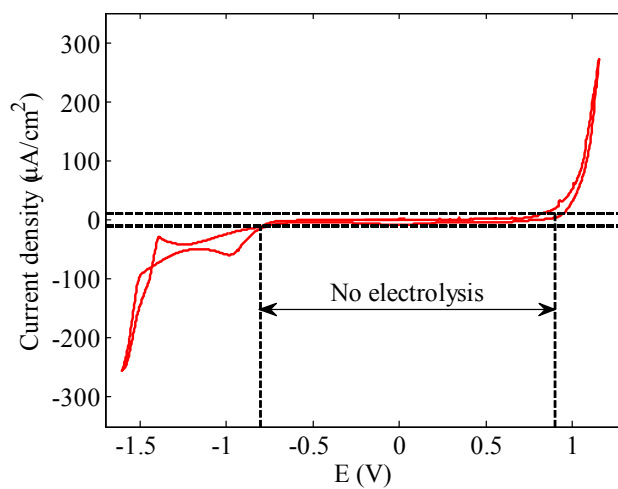
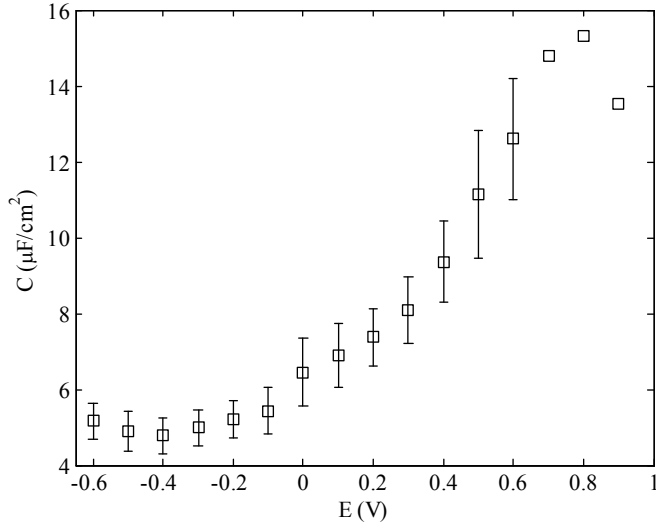


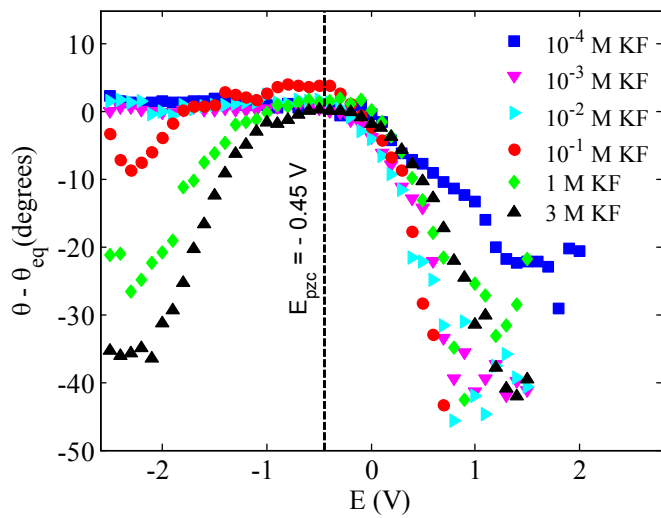
Supplementary Information: Ultra-low voltage electrowetting using graphite surfaces



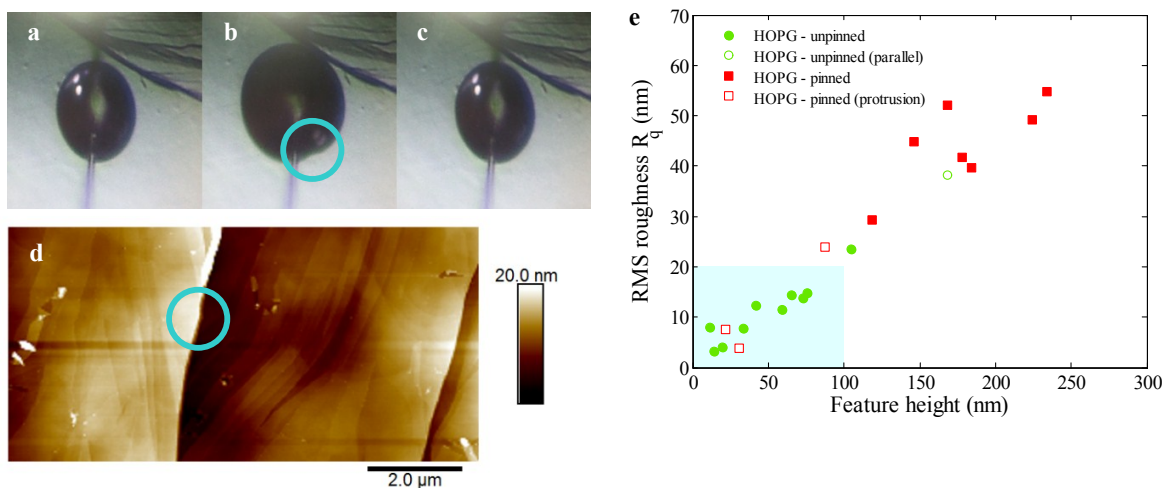
Supplementary Information figure 1: Cyclic voltammetric response for the 6 M LiCl/air system for $-1.6 \text{ V} < E < +1.2 \text{ V}$. The negative current flow seen at approximately -1.0 V is due to reduction of dissolved oxygen.



Supplementary Information Figure 2: Potential-dependent capacitance. Average capacitance ($n = 4$, error bars showing 1 standard deviation) of the HOPG/6 M LiCl(aq.) interface as a function of potential over the range used in Fig. 2. The error increases at higher potentials as the region of electrolysis is approached. This total capacitance was used to determine η in Fig 2(C), however the tail-off in the data at higher bias is attributed to the semi-metallic nature of graphite, which gives rise to its anomalously low, potential dependent capacitance.³¹ The total capacitance ($C(E)$) of the interface can be considered as the space charge (C_{SC}) and Helmholtz (C_H) capacitances in series, if one neglects the contribution from the diffuse double-layer at the high electrolyte concentration.³⁰ Accordingly, the potential has been corrected by the fraction of potential drop at the graphite surface, given by: $(1 - C(E) / C_{SC}) = C(E) / C_H$. In principle C_H can be obtained by measuring $C(E)$ at a metal electrode at the equivalent electrolyte concentration, however this assumes that C_H is constant and independent of substrate. Instead, we have treated C_H as a variable, $C_H(E)$, in our analysis of Fig. 2(C), and have found optimal agreement (see Inset, Fig. 2(C) with Eq. (6) when the maximum value of $C_H(E) = 30 \mu\text{F cm}^{-2}$, with C_H following the same potential dependence as the measured capacitance $C(E)$).

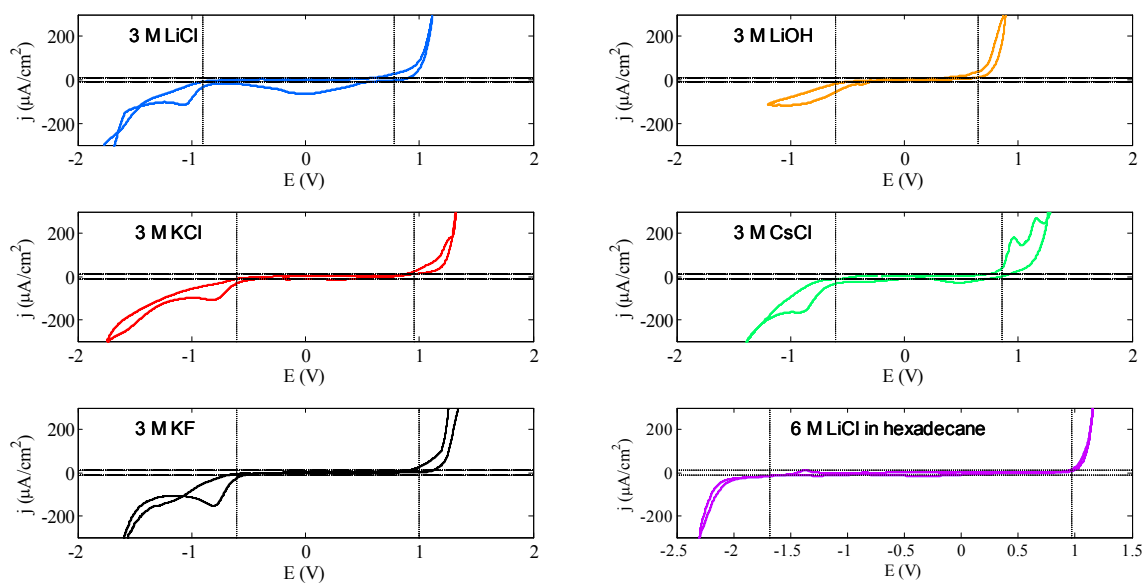


Supplementary Information figure 3: Effect of electrolyte concentration on EWOC. CA vs. potential dependence is illustrated for a range of potassium fluoride concentrations (10^{-4} M to 3 M).

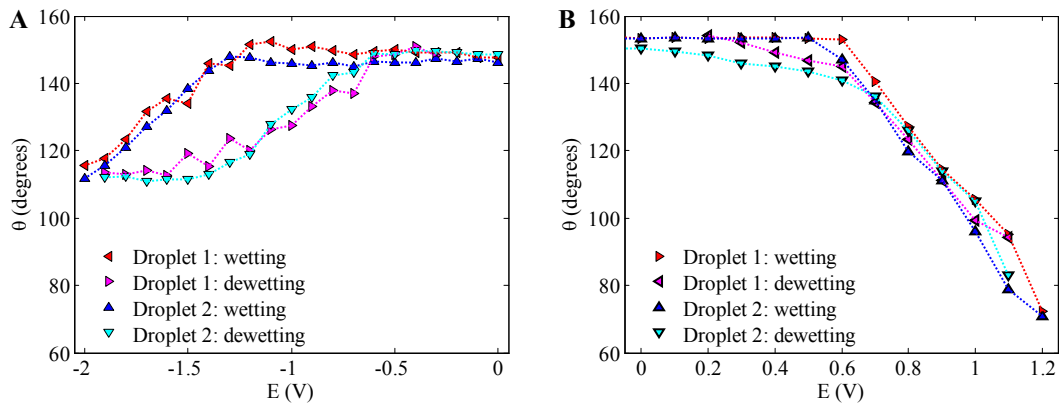


Supplementary Information Figure 4: Effect of surface defects on droplet pinning for aqueous/air

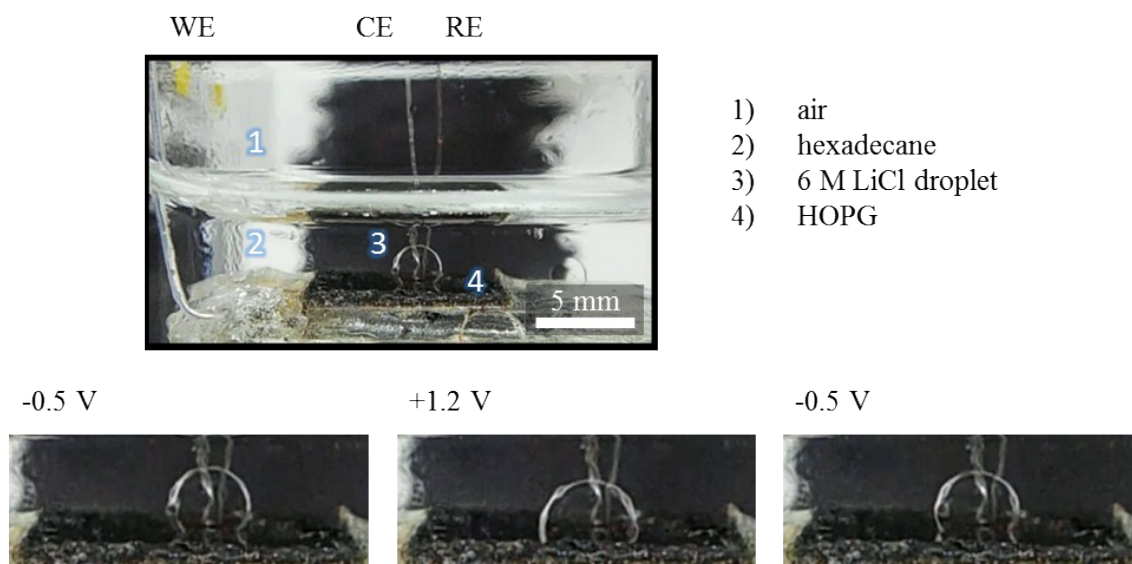
EWOC. (a) top-view image of a droplet at $E = -0.2$ V. (b) droplet at $E = +0.6$ V, note the “dimple” induced by the feature highlighted in the circle. (c) droplet on return to $E = -0.2$ V. (d) atomic force microscopy of the region of the HOPG where the droplet was deposited, the height of the step (circled in B, shown here at a slightly different orientation) is 30 nm. (e) The correlation between droplet pinning and steps exceeding approximately 20 nm in size, although the value of this threshold is contact angle (i.e. potential) dependent and also dependent on the orientation of the feature with respect to the direction of drop motion, with little effect found for features that were parallel to the advancing contact line.



Supplementary Information Figure 5: Cyclic voltammetric response for the various aqueous electrolyte solutions surrounded by air. **(a)** 3 M LiCl **(b)** 3 M LiOH **(c)** 3 M KCl **(d)** 3 M CsCl **(e)** 3 M KF **(f)** shows the response of a 6 M LiCl aqueous droplet on an electrode that was pre-soaked in hexadecane. The current data is plotted as current density, j , i.e. scaled by the area of the exposed graphite (see Methods). The increase in j for $E > +1.0$ V and $E < -1.5$ V (more negative in the case of **f**) indicates electrolytic breakdown of the solution, whereas the only electrolytic processes within this potential zone is due to oxygen reduction (also seen in Fig. S1, solutions were not degassed), showing a current peak at $E \approx -0.9$ V. The dashed horizontal lines indicate the current density we have defined as the onset of electrolysis, corresponding to $\pm 10 \mu\text{A cm}^{-2}$.



Supplementary Information Fig. 6: Reversibility and hysteresis of liquid-liquid electrowetting within the potential window where electrolysis does not occur. (a) Contact angle response for the negative branch as the potential was decremented/incremented in 0.1 V steps from/back to 0 V. Whilst the contact angle change is reversible on the return to potentials above -0.5 V, considerable hysteresis of 30° is observed. Note the bubble formation at the most negative potentials, see Fig. 1(c). (b) Contact angle response for the positive branch as the potential was incremented/decremented in 0.1 V steps from/back to 0 V. In contrast to the negative branch, the wetting and dewetting curves closely overlap, demonstrating the low level of hysteresis. The sudden onset of wetting suggests a threshold voltage must be overcome to enact a contact angle change. It is noteworthy that low CA hysteresis has been reported in the EWOD configuration with the use of similarly concentrated electrolyte systems, specifically ionic liquids and with less concentrated aqueous solutions³² however, the lack of hysteresis in these cases has been attributed to the use of a solid/liquid/liquid configuration where the surrounding liquid is assumed to form a microscopic film, lubricating motion of the droplet and minimising pinning effect due to imperfections in the solid.



Supplementary Information Fig. 7: EWOC with large droplets in the liquid/liquid configuration. (a)

Electrowetting was performed with 6 M LiCl droplets ($\sim 10 \mu\text{L}$) immersed in hexadecane, with the auxiliary electrodes (Pt wire CE and RE) placed in the electrolyte droplet. (b) The droplet response was recorded on alternating the potential between -0.5 V and $+1.2$ (4 s each) over several cycles. Rapid and reversible droplet wetting was observed, demonstrating that EWOC is not limited to microscale droplets.

A video file showing the dynamic response of the droplet (images present in **b**, above) is appended to the Supplementary Information.

Electrolyte	E_{pzc}/V	$\theta_{\text{eq}}/^\circ$	Electrolytic stability range/V
LiCl	-0.58 ± 0.05	62.2 ± 2.3	-0.95 to 0.90
LiOH	-0.12 ± 0.05	59.3 ± 8.6	-0.65 to 0.75
KCl	-0.48 ± 0.05	66.0 ± 5.2	-0.65 to 0.95
CsCl	-0.43 ± 0.05	62.2 ± 4.0	-0.65 to 0.90
KF	-0.45 ± 0.05	65.9 ± 1.6	-0.65 to 1.00

Supplementary Information Table 1: Summary of electrochemical and surface properties for aqueous electrolytes in air. Potential of zero charge, equilibrium contact angle (unbiased case) and range of electrolytic stability, defined as the region where the magnitude of the current density (i.e. current normalised to droplet area) was $< 10 \mu\text{A cm}^{-2}$. The data is an average of at least five experiments for each electrolyte.